

# Modeling Flow and Corrosion in Sweet Offshore Production

Madan Gopal  
Corrosion and Multiphase Technology Center  
Ohio University  
Athens, OH 45701

## Abstract

A systematic study of multiphase oil/water/gas flow and its effect on corrosion in industrial scale, large diameter horizontal and inclined pipes, has been carried out at high pressures and elevated temperatures. The results show that inclination affects the multiphase flow regime transitions dramatically. Slug flow is enhanced in upward flows with increased slug frequency and corrosion rates. No maximum has been observed in the corrosion over the range of temperatures investigated. The corrosion rate also increases with carbon dioxide partial pressure and Froude number. EIS has been shown to reveal information regarding the corrosion mechanisms on the surface. Increasing the iron content does not result in the protection of the pipe wall in slug flow. SEM micrographs reveal impact craters that damage the corrosion product layer, resulting in increased corrosion.

## Introduction

Multiphase transportation of oil/water/gas mixtures over long distance transportation lines is now a common feature in offshore production systems. The multiphase flow results in significant internal corrosion problems for carbon steel pipelines. Sweet corrosion involves carbon dioxide, which is present in the gas phase of the mixture. This can occur within the formation itself or be injected during enhanced oil recovery operations. The CO<sub>2</sub> dissolves in the water to form weak carbonic acid, which acts as the primary initiator of corrosion for carbon steel pipelines.

Several predictive models currently exist for sweet corrosion in oil and gas systems. De Waard and Milliams (1975) developed a corrosion model based on experiments carried out in stirred beakers. They reported that the corrosion rate increases with temperature from 30 C to 60 C, reaches a maximum between 60 C and 70 C, and thereafter decreases until 90 C. Later, an improved model incorporating correction factors for the non-ideality of carbon dioxide at higher pressures, formation of iron carbonate scales, and changes in pH and Fe<sup>2+</sup> ion concentration was developed (de Waard et al., 1991). Two subsequent revisions to the model were proposed. The first (de Waard et al., 1993) proposed a revised correlation between corrosion rate and flow velocity, temperature, and carbon dioxide partial pressure. The second (de Waard et al., 1995) proposed a semi-empirical model for corrosion rates.

Efird et al. (1993) proposed a correlation between shear stress and corrosion rate based on experiments in pipes, jet impingement apparatus, and rotating cylinder electrode systems. He also showed that pipe flow results compared better with jet impingement technique while rotating cylinder results grossly underpredicted the corrosion rates.

Jepson et al. (1996, 1997) proposed a corrosion model for multiphase slug flow that incorporated the effects of carbon dioxide partial pressure, temperature, water cut, slug flow turbulence through a pressure drop term, slug frequency, gas density, liquid viscosity, and crude oil type (through the product of acid number and percent nitrogen). This is currently the only predictive model developed for slug flow in carbon steel pipes.

Nesic et al. (1995) presented an electrochemical model for predicting carbon dioxide corrosion of carbon steel. The model included both the reductions of hydrogen ion and carbonic acid as the cathodic reaction, with the dissolution of iron as the anodic reaction. This electrochemical mechanism has been suggested by several other researchers and is now accepted as the governing mechanism for CO<sub>2</sub> corrosion.

Zhang et al. (1997) proposed a simplified transport model for the prediction of carbon dioxide corrosion of carbon steels in oil/water flows. A schematic of the model is shown in Figure 1. The dissolution of carbon dioxide in salt water together with the ions in the electrolyte determines the bulk composition of hydrogen ions and the pH of the solution. In the simplified model, only the transport of hydrogen to and ferrous ions from the corroding surface is considered. The effect of the multiphase flow is primarily felt within the mass transfer layer, the characteristics of which determine the corrosion rate for a given chemistry. A further refinement of the model is presented in Figure 2. Here, the corrosion product layer is allowed to build up and transport of hydrogen and ferrous ions through this layer is considered as well. Currently research at the Center is aimed at determining the effect of multiphase slug flow on structure of this layer and the consequent effect on mass transfer.

Figure 3 describes schematically, the various flow regimes observed in multiphase gas/oil/water flows. The corresponding flow regime transition maps for horizontal and inclined flows are shown in Figures 4 and 5.

At low liquid and gas velocities, there is little interfacial friction between the three phases. Consequently, gas, oil, and water flow in stratified layers, with gas at the top, oil in the middle, and water at the bottom of the pipe. This can occur in "dead zones" in the system. The interfaces between the phases are smooth. This is smooth stratified flow. With increasing gas velocity, waves appear at the gas/oil interface due to increasing interfacial friction. Some of the momentum is transferred through the oil layer into the oil/water interface, and the droplets of oil in water, or water in oil begin to appear. This is wavy stratified flow. Upon increasing the gas velocity even further, the waves at the gas/oil interface begin to roll over and acquire a three dimensional character. This flow regime is called roll waves. If the liquid velocity is increased, at low gas velocity, lumps of liquid flow over the stratified oil/water layers without any turbulence or mixing. This is plug flow and is only of minor importance. If the gas velocity is now increased, the

front of the intermittent plug begins to accelerate and begins to assimilate slow moving liquid ahead of it. The front of the slug resembles a wave breaking on a sea beach and creates a highly turbulent, frothy mixing zone behind it. Large amounts of gas is assimilated into the mixing zone and released into the slug in the form of pulses of bubbles. These pulses of bubbles are forced towards the bottom of the pipe, where they do impact and can collapse, causing a cavitation-type damage. It is this unique multiphase flow characteristics of slug flow that causes dramatic increases in the corrosion rate. The extent of the corrosion damage is related to the intensity of turbulence and length of the mixing zone of the slug and the frequency of slugs. As the velocity is increased even further, the amount of gas entrained increases within the slug and ultimately blow-through occurs, and the gas now flows in a central core in the pipe with an annulus of liquid around the pipe. This is annular flow.

It can be seen from Figure 4 that slug flow is the dominant flow regime even in horizontal pipes. Figure 5 shows the effect of inclination on the multiphase flow regime transitions. It is seen that in upward inclined pipes, stratified flow is completely eliminated and slug flow dominates the flow map. Even an inclination of  $0.5^\circ$  results in the elimination of stratified flow from the map within the range of flow rates of interest in oil and gas production.

Jepson (1987) showed that slugs were hydraulic jumps. He observed that the gas was entrained into the slugs in the form of pulses of bubbles. He characterized the intensity of the slugs using a dimensionless Froude number as follows:

$$Fr = (V_t - V_{LF}) / \sqrt{gh_{EFF}} \quad (1)$$

Where,

Fr	=	Froude number in the film ahead of the slug
$V_t$	=	Translational velocity of the slug
$V_{LF}$	=	Film velocity ahead of the slug
$h_{EFF}$	=	Effective height of the liquid film

Zhou and Jepson (1994) and Gopal et al. (1995) discussed possible mechanisms contributing to enhanced corrosion in pipes in multiphase slug flows. It was found that there existed a strong correlation between void fraction at the bottom of the pipe and the corrosion rate. The void fraction in turn could be correlated to the film Froude number ahead of the slug and the pressure drop across the slug. The turbulent intensity of the slug increases with Froude number.

## EXPERIMENTAL SETUP

A predetermined amount of oil and saltwater are stored in a  $1.5 \text{ m}^3$  stainless steel tank and is pumped by a 1.5 kW high pressure, stainless steel, centrifugal pump into a 7.5 cm diameter stainless steel pipe, where the liquid flow rate is measured using turbine flow meters. Carbon dioxide gas from a 20-ton, high pressure storage tank is introduced into

the system and its flow rate is measured using inline, magnetic flow meters. The gas/oil/water mixture then flows through a 10-cm diameter, 40-m long, high pressure, high temperature, fully inclinable, stainless steel pipe, where all the multiphase flow and corrosion measurements are made. The multiphase mixture then flows through a 10-cm diameter pipe and is recycled into the system by a unique, Moyno, triphaze pump that can handle up to 99% gas. The 40-m length is divided into two 20-m sections with an inline separator. Both upward and downward flows can be studied simultaneously using this system. The system can be operated up to 150 bars and a temperature of 150 C. A schematic of the system is shown in Figure 6.

## TEST SECTION

Figure 7 shows a schematic of the test section. The test section consists of a 10-cm diameter, 2-m long, stainless steel pipe with ports for inserting corrosion probes and for measurement of multiphase flow characteristics including, phase and velocity profiles across the vertical diameter and pressure drop due to the flow.

There are two ports each (E) at the top and bottom of the pipe for inserting electrical resistance (ER) probes for corrosion measurement. The probes are mounted flush with the inside pipe wall to allow determination of corrosion rate at the six and twelve o'clock positions. Electrochemical probes such as electrochemical impedance spectroscopy (EIS), electrochemical noise (ECN), and DC polarization can also be used. Limiting current density values (LCD) from DC polarization experiments can be used to determine a mass transfer coefficient that can be correlated to pressure drop and shear stress.

The test section has several pressure taps (C) to measure the instantaneous pressure gradient at different distances in the flow. A patented non-visual technique to determine multiphase flow regimes based on pressure drop and velocity measurements has been developed at the Center using these ports. D is a pressure port that can also be used to insert a flush-mounted, hot film probe to determine instantaneous wall shear stress. This can then be correlated to the pressure drop. A sampling port (A) is used to insert a pitot tube into the test section and determine instantaneous velocity profiles in the multiphase flow. The tube can also be used to withdraw isokinetic samples of the flowing mixture to determine flow characteristics such as oil/water fractions, holdup of liquid and gas, and height of the liquid film in stratified flow. The iron and oxygen contents of the solution can also be monitored using this port. Details of the multiphase flow systems and the experiments carried out have presented in several previous papers (e.g., Sun and Jepson, 1992, Jepson et al., 1996, Maley, 1997a).

Also, a patented, noninvasive, ultrasonic multiphase flow and corrosion measurement system is currently under development at the Center to determine flow characteristics such as film height distribution, holdup variation, and average phase velocities and metal thickness loss down to 10 microns. The current state-of-the-art is 25 microns using the Field Signal Method (FSM). The ultrasonic corrosion measurement system is also being designed to determine corrosion mechanisms using special mathematical analysis of the received signals.

## TEST MATRIX

Table 1 shows the experimental test matrix used to determine the corrosion and multiphase flow results presented in this paper. ASTM substitute seawater was used for the aqueous phase. Two different oils were used to make up the oil/water mixtures in the liquid phase. One was similar to a light crude with a viscosity of 2 cp and the second was similar to a moderately viscous crude with a viscosity of 100 cp. Carbon dioxide and a mixture of carbon dioxide and nitrogen have been used in the gas phase.

Table 1: Test Matrix

Water	:	ASTM substitute seawater
Water cut	:	20%, 40%, 60%, 80%, 100%
Oils	:	LVT200 ( $\mu = 2$ cp, $\rho = 800$ kg/m <sup>3</sup> ) Britol150T ( $\mu = 100$ cp, $\rho = 825$ kg/m <sup>3</sup> )
Gas	:	Carbon dioxide, nitrogen
Pressure	:	0.26, 0.45, 0.79 MPa
Temperature	:	40, 60, 80, 90 C
Pipe inclination	:	0°, ± 2°, ± 5°
Liquid velocity	:	0.1 – 2 m/s
Gas velocity	:	1 – 8 m/s
Froude number	:	6, 9, and 12

## RESULTS

### *Effect of Temperature on Corrosion*

The variation of corrosion rate with temperature at different carbon dioxide partial pressures and Froude numbers is shown in Figure 8 for 100% saltwater in the liquid phase for horizontal flow. The gas phase consisted of only carbon dioxide in this case.

It is seen that the corrosion rate increases over the entire range of temperatures for all the conditions of pressures and Froude numbers. For example, at a pressure of 0.45 MPa at Froude number 9, the corrosion rate increases from about 11 mm/yr at 40 C to 32 mm/yr at 60 C, and then on to about 63 mm/yr. at 90 C. No maximum is seen in the corrosion

rates over the entire range of temperature studied. This is contrary to the prediction by de Waard and Milliams (1975). This is true for all multiphase flow-enhanced sweet corrosion of carbon steel. Figure 9 shows the variation of corrosion rate with temperature for 80% water cut and the results are similar to those of Figure 8. No maximum in corrosion is observed, and the corrosion rate increases with temperature at all carbon dioxide partial pressures and for all Froude numbers. For example, at a carbon dioxide partial pressure of 0.27 MPa at Froude number 12, the corrosion rate increases from about 8.2 mm/yr. at 40 C to about 12.5 mm/yr. at 60 C, and then on to 19.5 mm/yr. at 80 C. Detailed description of these results are given in Bhongale (1996).

### *Slug Flow Characteristics*

Slug flow involves unique multiphase characteristics not seen in other flow regimes, as described earlier. The turbulent mixing zone involves entrainment of large amounts of gas, which is released into the slug in the form of pulses of bubbles that are forced towards the bottom of the pipe. The frequency and turbulent intensity of the pulses of bubbles increases with Froude number and these mechanisms have been described in earlier papers (Gopal et al., 1995). The gas bubbles do impact and can collapse on the pipe wall, causing the corrosion product to be removed from surface and enhancing localized corrosion.

The effect of the turbulence of these pulses of bubbles on wall shear stress, pressure drop, and mass transfer is shown in Figures 10, 11, and 12.

Figure 10 shows the variation of instantaneous wall shear stress within the mixing zone of the slug at a Froude number of 14 for 100% water cut. Details of the measurements and the discussion of the results can be found in Maley (1997b). It is seen that fluctuations of about 40 Pa around an average shear stress value of 120 Pa are seen at regular frequencies. The intensities and frequency of these fluctuations have been shown to increase with Froude number (Maley, 1997b). Fourier analysis shows the frequencies to correspond with those of the pulses of bubbles in the mixing zone observed visually.

Figure 11 presents the results of the instantaneous pressure fluctuations within the mixing zone of the slug at the same conditions as Figure 10. It can be seen that fluctuations similar to those seen in the wall shear stress occur here as well. Pressure fluctuations of about 4000 Pa are seen at regular intervals about a mean value of 2000 Pa. The frequency of the fluctuations is similar to those seen in Figure 10.

The pressure and shear stress results can be correlated for slug flow. It has been suggested by Efirid (1993) that the effect of flow on corrosion can be quantified using the wall shear stress. Since the shear stress is both difficult to measure and calculate for slug flow, the correlation between wall shear and pressure drop has allowed the use of pressure gradient as a function of Froude number in a predictive corrosion model developed at the Center. The pressure drop then indicates the level of gas entrainment within the mixing zone and the consequent turbulent intensity associated with it.

The results from mass transfer measurements using limiting current density measurements in slug flow at a Froude number of about 12 are shown in Figure 12. Details of these results have been presented elsewhere (Jiang and Gopal, 1998a and b). Peaks at regular intervals are observed. For example, at times of 1, 1.5, 3 and 3.5 s, peaks ten times the average value are seen. At time instants of 1.25, 3.25 and 3.75 s, peaks 100 times the average value, are observed. Again, the large amplitude fluctuations around a mean value are indicative of the impact of gas bubbles on the electrode surface within the mixing zone of the slug. Work is currently going on at the Center to correlate mass transfer with Froude number and slug frequency to predict the effect of multiphase slug flow on the transport of corrosive species to the pipe wall and consequently its effect on corrosion rate.

A three-dimensional video image of the mixing zone of the slug is captured in Figure 13. The large amount of gas entrained within the slug is clearly understood from this image. It is also easily seen that the entrained gas is forced towards the bottom of the pipe as the front of the slug rolls over and assimilates slow moving liquid and gas ahead of it. The results from Figures 10, 11, and 12 can be explained as above in the light of this image.

#### *Effect of Liquid Viscosity*

The effect of liquid viscosity on the sweet corrosion rate in multiphase flows is described in Figure 14. It is seen that the corrosion decreases significantly as the viscosity increases from 2 to 8 cp and then slowly as the viscosity increases further to about 20 cp. For example, at 0.79 MPa at Froude number 12, the corrosion rate decreases from 23.5 mm/yr. to 17 mm/yr. as the viscosity increases from 2 to 8 cp and then to 12 mm/yr. with a decrease in viscosity to 20 cp.

As the liquid phase viscosity increases, the level of turbulence within the mixing zone decreases. This is shown by the reduction of pressure drop across the slug. This results in less entrainment of gas and less shear at the wall of the pipe. This results in less erosion of the corrosion product layer and less corrosion.

#### *Effect of Gas Density*

The effect of multiphase slug flow on corrosion can also be described using gas density as a variable. As the carbon dioxide partial pressure increases, the corrosion rate increases due to a pH effect, which is well known. However, with increase in system pressure, there is an increase in gas density, which increases the turbulence and wall shear stress associated with the pulses of bubbles.

Figure 15 shows the effect of gas density on the corrosion rate in slug flow. The figure compares corrosion rate at a total system pressure of 0.79 MPa. In one case, the gas phase consists solely of carbon dioxide and in the second case, a mixture of carbon dioxide and nitrogen is used. The partial pressure of carbon dioxide in the second case is 0.27 MPa. It is seen that corrosion rate increases because of gas density at the same pH. For example, the corrosion rate at 0.27 MPa partial pressure of pure carbon dioxide at a Froude number of 9 at 80 C is 5.8 mm/yr. With the carbon dioxide partial pressure kept constant (i.e.

same pH), when the total pressure is increased to 0.79 MPa, the corrosion rate increases to 8.1 mm/yr. This is lower than the value of 14.2 mm/yr obtained with 0.79 MPa pure carbon dioxide pressure, but still shows a significant increase over the baseline corrosion rate. Similar results are seen at Froude number 12.

### *Froude Number Effects*

Figure 15 also shows the effect of increasing Froude number on corrosion rate. At 60 C with a carbon dioxide partial pressure of 0.79 MPa, the corrosion rate increases from 10.1 mm/yr to 13.2 mm/yr. as the Froude number is increased from 9 to 12. Increasing the Froude number results in increased turbulence and gas entrainment within the mixing zone of the slug. This results in higher wall shear stress and pressure drop across the slug with associated increases in the corrosion rate.

### *Effect of Inclination*

As mentioned earlier, inclining a pipe by even half a degree can cause the elimination of stratified flow in upward multiphase flow and a dominant slug flow regime can occur. Also, owing to gravity effects, the height of the liquid film increases, resulting in an increase in the slug frequency. Further, rollback of liquid down the pipe, can result in an increase in the Froude number. Both effects contribute to increase the corrosion rates in upward inclined pipes. In downward flow, the dominant flow regime is stratified.

The variation of Froude number with superficial gas velocity for various superficial liquid velocities is shown in Figure 16. It is seen that the Froude number increases linearly with gas velocity. This is expected since, at higher gas velocities, the in situ gas velocity controls the slug translational velocity, and the liquid velocity is not much different. It should be noted from Figure 16 that slug flow with Froude numbers close to 5 can be observed even at liquid velocities as low as 0.1 m/s and gas velocities less than 2 m/s in upward inclined pipes.

Jepson and Taylor (1988) proposed a correlation for slug frequency in horizontal flow. Figure 17 compares the observed average slug frequency in 2° and 5° upward flows with their correlation as a function of the mixture velocity. It can be seen that upward inclination results in significant increases in slug frequency. A generalized correlation for slug frequency as a function of inclination has been developed at the Center.

The effect of slug frequency on corrosion rates at two different Froude numbers is shown in Figure 18 for 2° upward flows at a carbon dioxide partial pressure of 0.27 MPa. It can be seen the corrosion rate increases approximately linearly with slug frequency up to about 35 slugs/min. It then tends to remain constant with increasing slug frequency. For example, with 20% oil at Froude number 12, the corrosion rate increases linearly from about 4.1 mm/yr. to 7.5 mm/yr. with increase in slug frequency from 6 slugs/min to 34 slugs/min and remains at approximately the same value at a higher frequency of 44 slugs/min. Similar results are seen at other Froude numbers, water cuts, pressures and temperatures.

With increasing slug frequency, the effect of the turbulence of the mixing zone on the corroding surface increases. At lower slug frequencies, the product film along with any inhibitor may have a chance to repair itself before encountering a second slug. At higher slug frequencies, this repair process is hindered and at a critical frequency of about 35 slugs/min, the effect of the turbulence of the mixing zone becomes permanent and further increases in slug frequency have little effect.

#### *Corrosion Rate Model*

Based on the extensive database of corrosion and multiphase slug flow characteristics generated at the Center, a predictive model for sweet corrosion of carbon steel in slug flow has been developed. The model includes separate terms for carbon dioxide partial pressure, temperature (these determine the pH of the system), water cut, pressure drop across the slug (which is a direct function of Froude number), gas density, liquid viscosity, and slug frequency. Based on the results of Eford (1989), the model also includes the effect of crude oil based on the acid number and percent nitrogen of the crude. The model is available to member companies.

#### *Electrochemical Methods*

The corrosion mechanisms in multiphase flows and the effect of the flow on inhibitor performance can be determined using different electrochemical techniques. These are being developed at the Center and the details are given elsewhere (Chen, 1998 a,b).

Figure 19 depicts the electrochemical impedance spectroscopy (EIS) Nyquist plot for an inhibitor used in 100% salt water. The equivalent circuit used to fit the experimental data to a model is also shown. It is seen that a uniform film of inhibitor exists on the corrosion surface and the resulting circuit can be described with one surface resistance with one time constant. The increasing diameter of the semi-circle shows higher resistance to corrosion which is indicative of a protective film. This can then be compared to the spectra seen in Figure 20, which shows the result for an inhibited surface exposed to slug flow at Froude number 9. Here, a combination of a one time-constant resistance with a Warburg diffusion element in the electrical circuit is needed to describe the surface behavior. The reason is the disruption of the uniformity of the film due to slug flow. The pulses of gas bubbles described earlier, upon impact and possible collapse on the surface, possess enough energy to rupture binding of the inhibitor/corrosion product layer with the metal surface. This can result in "holes" or impact craters on the layers which can allow diffusion of the corrosive species to the metal surface resulting in degradation of the inhibitor.

#### *Effect of Iron*

It has been suggested, following de Waard and Milliams, that under certain conditions, the iron carbonate corrosion product layer, may become protective and prevent further corrosion. These conditions have been termed "scaling conditions".

Figure 21 shows a comparison of corrosion rates in slug flow under conditions of negligible iron in the solution with dissolved iron increased to the limit of negligible corrosion under oil/water full pipe flow conditions. It can be seen that increasing the iron concentration in the solution has resulted in a decrease in corrosion but it is not negligible under slug flow. For example, at a carbon dioxide partial pressure of 0.79 MPa, the corrosion rate for Froude number 6 with no iron is 28 mm/yr. and increases to 33 mm/yr. at Froude number 12. The corresponding rates are 13.5 mm/yr. and 16 mm/yr. with 95 ppm dissolved iron.

### *Surface Analysis*

The reason for the continued corrosion of carbon steel in slug flow, even under “scaling conditions” can be seen from Figures 22 and 23. Figure 22 shows the corrosion surface under full pipe oil/water flow conditions. It is seen that the surface is covered with a uniform film of corrosion product. It is densely packed and consequently fully protective. When this surface is compared with the one shown in Figure 23, which shows the corrosion layer exposed to slug flow, it is seen that parts of the layer have been removed revealing “holes” with the underlying metal surface being exposed. This is typical of the damage caused by slug flow due to the impact and possible collapse of the gas bubbles in the mixing zone. In some cases, the corrosion product layer is removed completely from the surface. Details of this study will be presented elsewhere (Gopal and Rajappa, 1999).

### **Conclusions**

A detailed study on the effect of multiphase flows on sweet corrosion of carbon steel pipes has been carried out at pressures up to 0.79 MPa and temperature up to 90 C. Multiphase flow has been shown to have a dramatic effect on corrosion rates of carbon steel.

Slug flow is the dominant flow regime in multiphase pipelines. Stratified flow is eliminated even at inclinations of  $0.5^\circ$ . This results in dramatic increases in corrosion rates.

Slug flow involves unique mechanisms with large amounts of gas entrainment within the liquid slug. The gas is released within a turbulent mixing zone in the form of pulses of bubbles that are forced towards the bottom of the pipe. The bubbles do impact and possibly collapse on the pipe surface causing a cavitation-type effect, which results in significant localized corrosion. The turbulence and frequency of these pulses of bubbles is a strong function of the Froude number in the film ahead of the slug.

Froude number and slug frequency increase due to gravity effects in upward inclined flows, thereby increasing corrosion.

The corrosion increases linearly with slug frequency until about 35 slugs/min and then remains constant.

No maximum is seen in corrosion rates with increasing temperature over the range studied. Corrosion also increases with carbon dioxide partial pressure and Froude number.

The corrosion rate decreases with increasing viscosity due to a reduction in turbulence.

Gas density does have a separate mechanical effect on the corrosion rate in slug flow due to the pulses of bubbles in the mixing zone.

Shear stress, turbulent intensity, pressure drop, and mass transfer measurements all show similar fluctuations at regular time intervals within the mixing zone of the slug. This supports the visual observations about the pulses of bubbles within the mixing zone.

EIS technique is able to detect corrosion mechanisms and equivalent circuit models predict the existence of a uniform or damaged film on the corroding surface.

A predictive model for corrosion of carbon steel in slug flow has been developed. The model includes the effect of carbon dioxide partial pressure, temperature, pressure drop across the slug, water cut, gas density, oil viscosity, slug frequency, and crude oil type.

Increasing the iron content beyond saturation limits to reach scaling conditions does not protect the pipe from further corrosion in slug flow. SEM micrographs show impact craters consistent with bubble impact that cause severe damage to the corrosion product layer, resulting in continued localized corrosion.

## References

1. Bhongale, S., "Effect of Pressure, Temperature, and Froude Number on Corrosion under Horizontal Multiphase Flow", M.S. Thesis, Ohio University, 1996.
2. Chen, Y., and Gopal, M., "Electrochemical Methods for Determining Corrosion Inhibition Mechanisms in Multiphase Flows," Corrosion/99, paper no. 509, (Houston, TX: NACE International, 1999).
3. Chen, Y. Chen, H., and Jepson, W. P., "Effect of Multiphase Flow on Corrosion Inhibition", Corrosion/99, paper no. 12, (Houston, TX: NACE International, 1999).
4. De Waard C., and Milliams, D. E., "Carbonic Acid Corrosion of Steel", Corrosion, 31, 5 (1975): p. 177.
5. De Waard, C., Lotz, U., and Milliams, D. E., "Predictive Model for CO<sub>2</sub> Corrosion Engineering in Wet Natural Gas Pipelines", Corrosion, 47, 12 (1991): p. 76.
6. De Waard, C., Lotz, U., and Dugstad, D., "Influence of Liquid Flow Velocity on CO<sub>2</sub> Corrosion: A Semi-Empirical Model," Corrosion/95, paper no. 128, (Houston, TX: NACE International, 1995).
7. Efird, D. E., "Effect of the Crude Oil on the Corrosion of Steel in Crude oil/Brine Production", Corrosion, 45, 2, Feb. 1989.
8. Efird, K. D., Wright, E. J., Boros, J. A., and Hailey, T. G., "Wall Shear Stress and Flow Accelerated Corrosion of Carbon Steel in Sweet Production", 12<sup>th</sup> International

- Corrosion Congress, Technical paper TS 14 194, (Houston, TX: NACE International, 1993).
9. Gopal, M., Kaul, A., and Jepson, W. P., "Mechanisms Contributing To Enhanced Corrosion in Three Phase Slug Flow in Horizontal Pipes", Corrosion/95, paper no. 105, (Houston, TX: NACE International, 1995).
  10. Gopal, M., and Rajappa, S., "Effect of Multiphase Slug Flow on the Stability of Corrosion Product Layers," Corrosion/99, paper no. 46, (Houston, TX: NACE International, 1999).
  11. Jepson, W. P., "The Flow Characteristics in Horizontal Slug Flow", 3<sup>rd</sup> Int. Conf. On Multiphase Flow", Paper F2, 187 (1987).
  12. Jepson, W. P., and Taylor, R. E., "Slug Flow and its Transitions in Large Diameter Horizontal Pipes", AERE-R12992, Harwell Laboratories, U.K., 1988.
  13. Jepson, W. P., Bhongale, S., and Gopal, M., "Predictive Model for Sweet Corrosion in Horizontal Multiphase Slug Flow", Corrosion/96, paper no. 19, (Houston, TX: NACE International, 1996).
  14. Jepson, W. P., Stitzel, S., Kang, C., and Gopal, M., "Model for Sweet Corrosion in Horizontal Multiphase Slug Flow", Corrosion/97, paper no. 602, (Houston, TX: NACE International, 1997).
  15. Jiang, L., and Gopal, M., "Calculation of Mass Transfer in Multiphase Flow", Corrosion/98, paper no. 50, (Houston, TX: NACE International, 1998).
  16. Maley, J., "Slug Flow Characteristics and Corrosion Rates in Inclined, High Pressure, Multiphase Flow Pipes", M.S. Thesis, Ohio University, 1997.
  17. Maley, L., "A Study of Slug Flow Characteristics in Large Diameter, Horizontal Multiphase Pipelines", M.S. Thesis, Ohio University, 1997.
  18. Nestic, S., Postlethwaite, J., and Olsen, S., (1995), "An electrochemical model for prediction of CO<sub>2</sub> Corrosion", Corrosion/95, paper no. 131, (Houston, TX: NACE International, 1995).
  19. Sun, J-Y, and Jepson, W. P., "Slug Flow Characteristics and their Effect on Corrosion Rates in Horizontal Oil and Gas Pipelines", SPE 1992, paper no. 24787, (Houston, TX: SPE, 1992).
  20. Zhou, X., and Jepson, W. P., "Corrosion in Three-Phase Oil/Water/Gas Slug Flow in Horizontal Pipes", Corrosion/94, paper no. 26, (Houston, TX: NACE International, 1994).

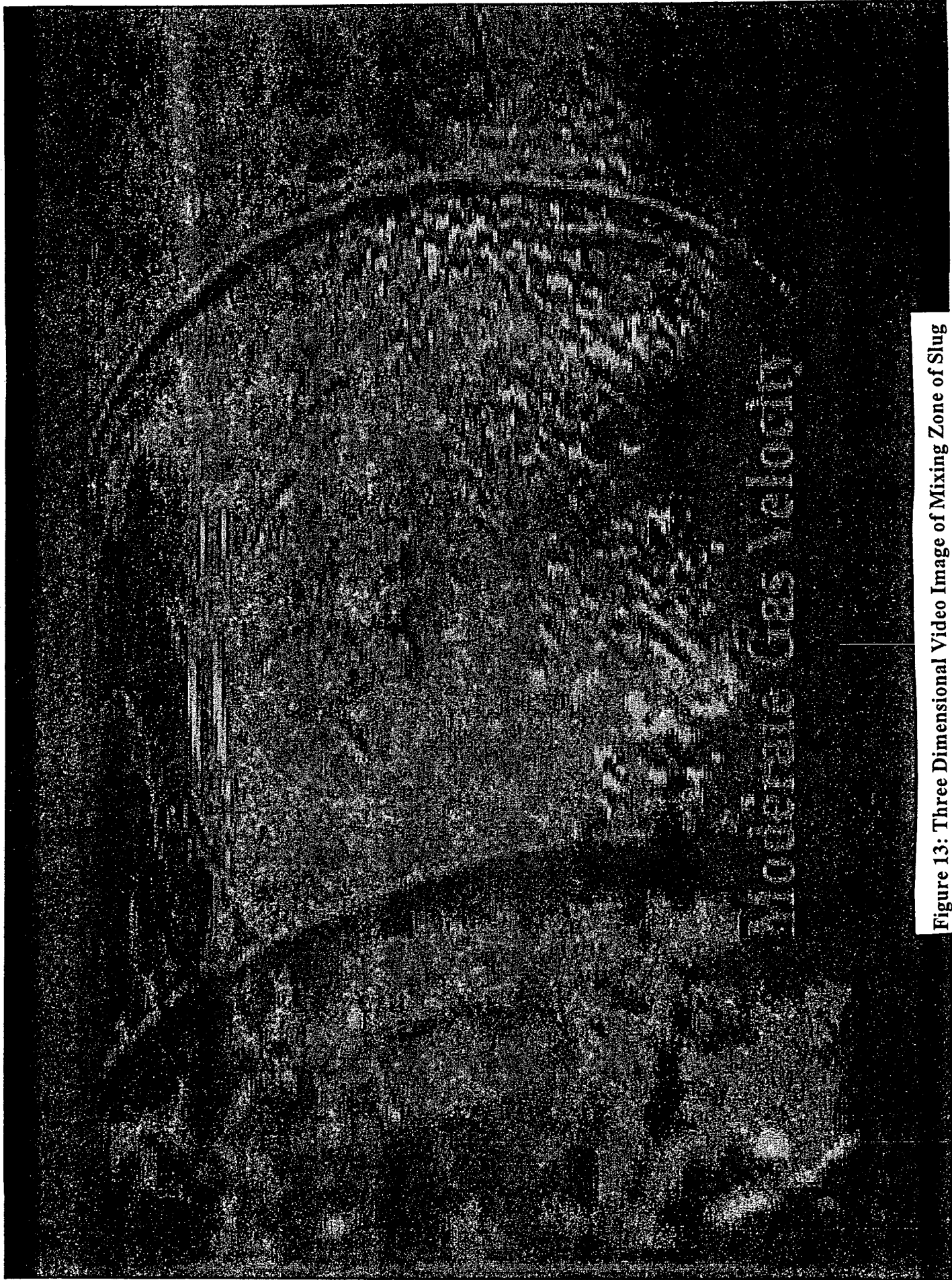
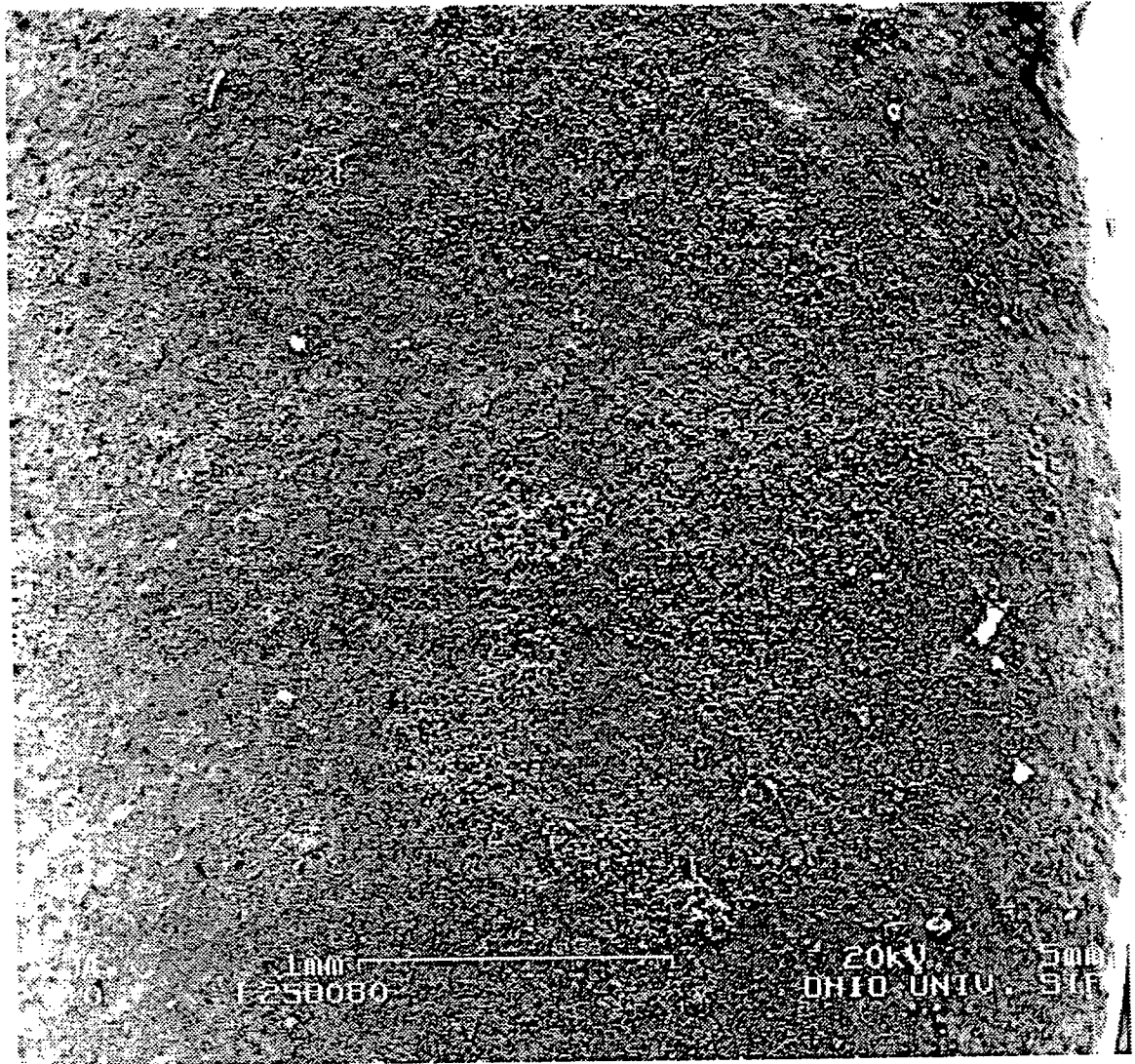
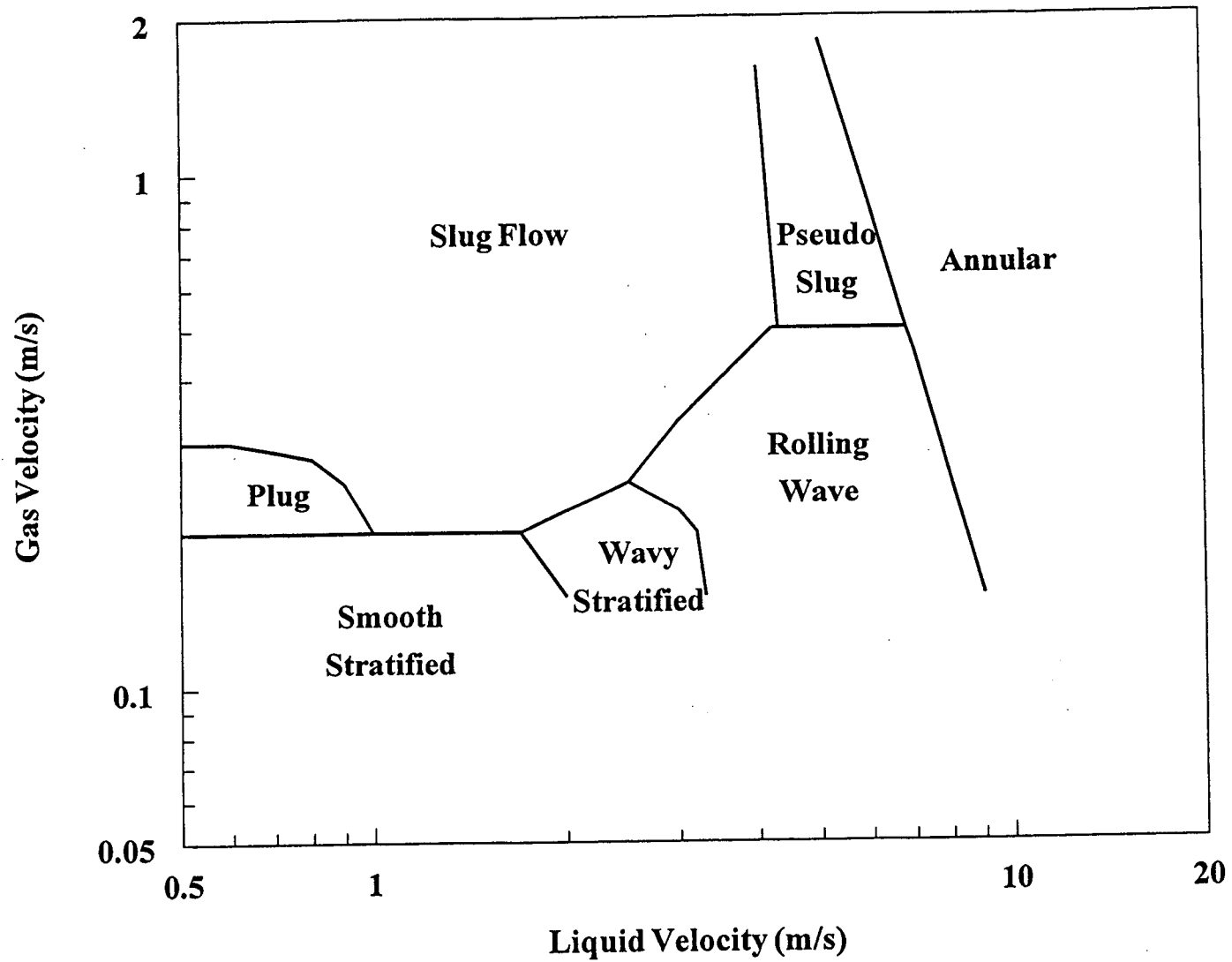


Figure 13: Three Dimensional Video Image of Mixing Zone of Slug



**Figure 22: Surface of Corrosion Coupon Exposed to full pipe oil/water flows**



**Figure 4: Flow regime map for multiphase horizontal flow**



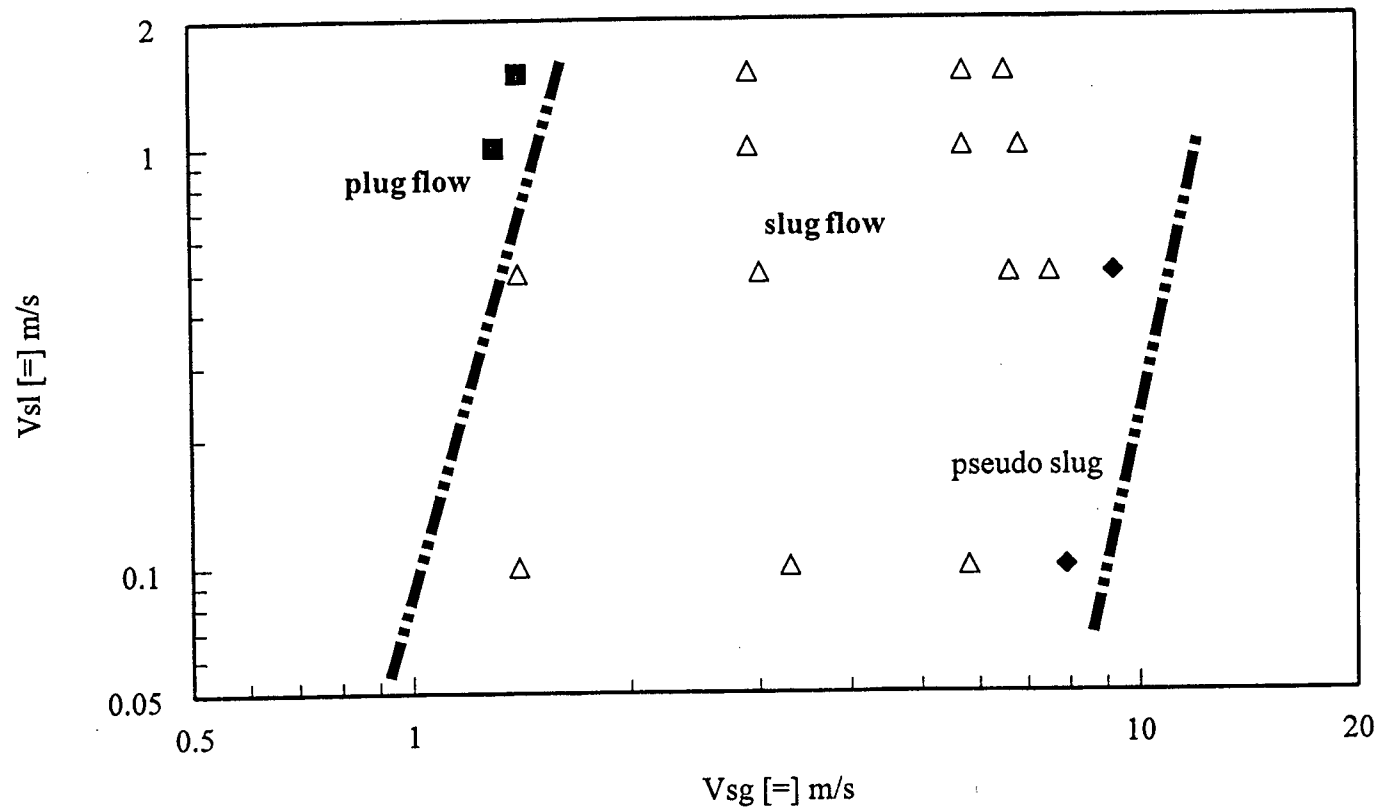
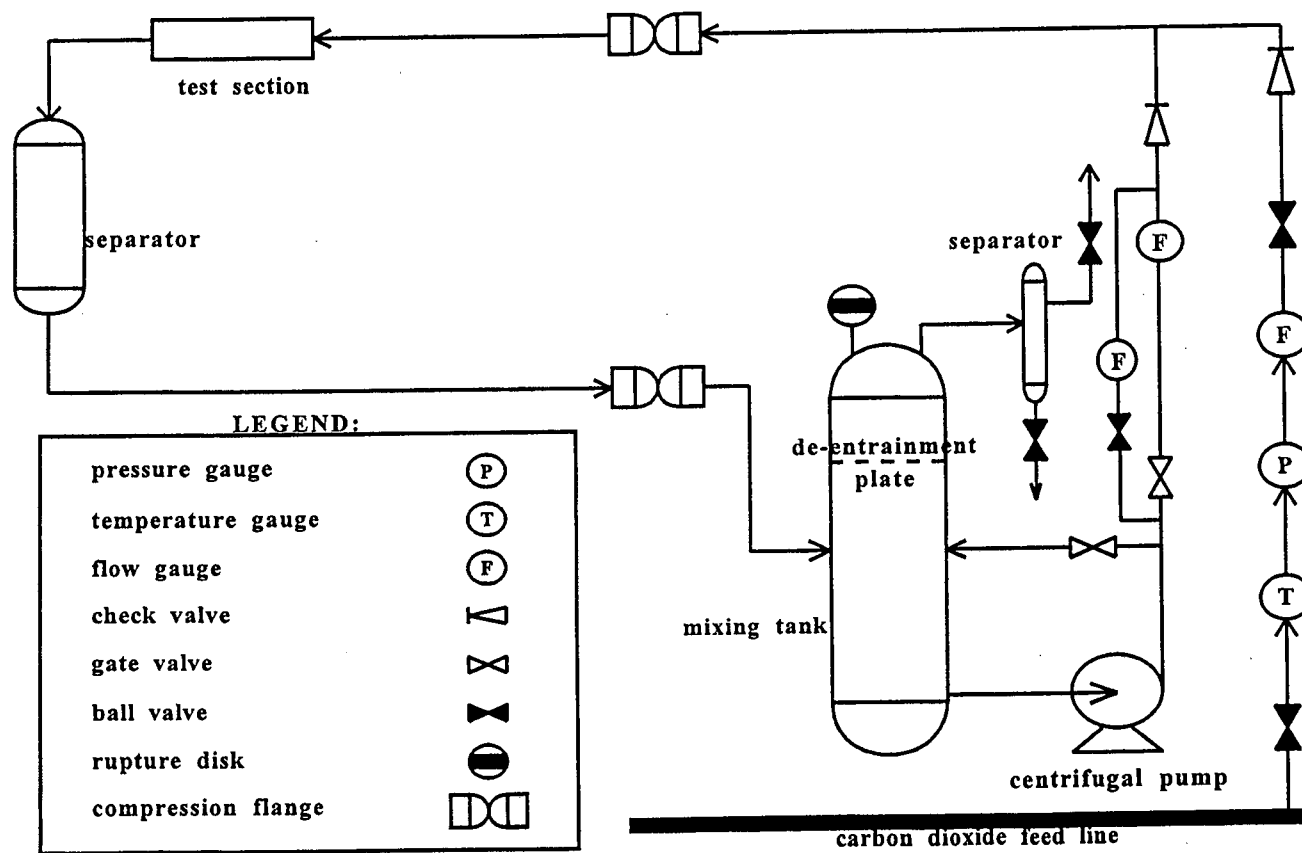
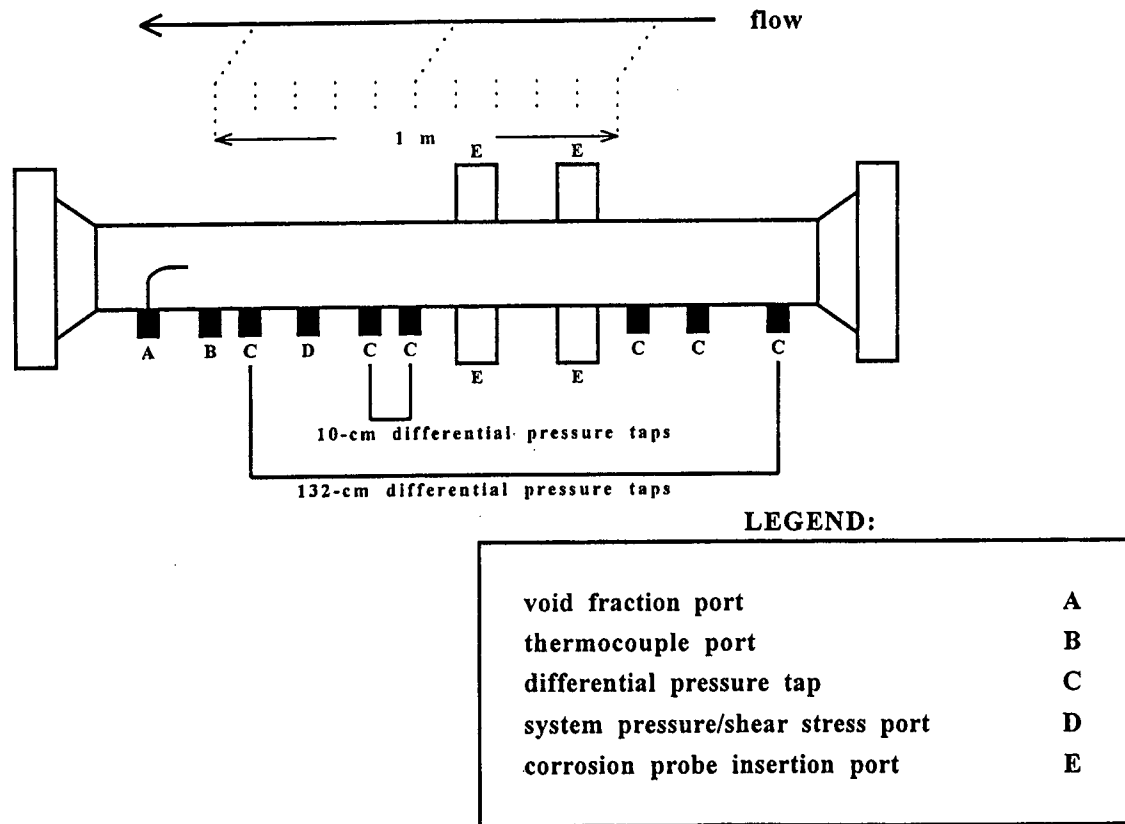


Figure 5: Flow regime map for 40% ASTM seawater, 2° inclination, 0.27 MPa



**Figure 6: High-pressure, inclinable flow system process flowsheet.**



**Figure 7: Schematic of Test section.**

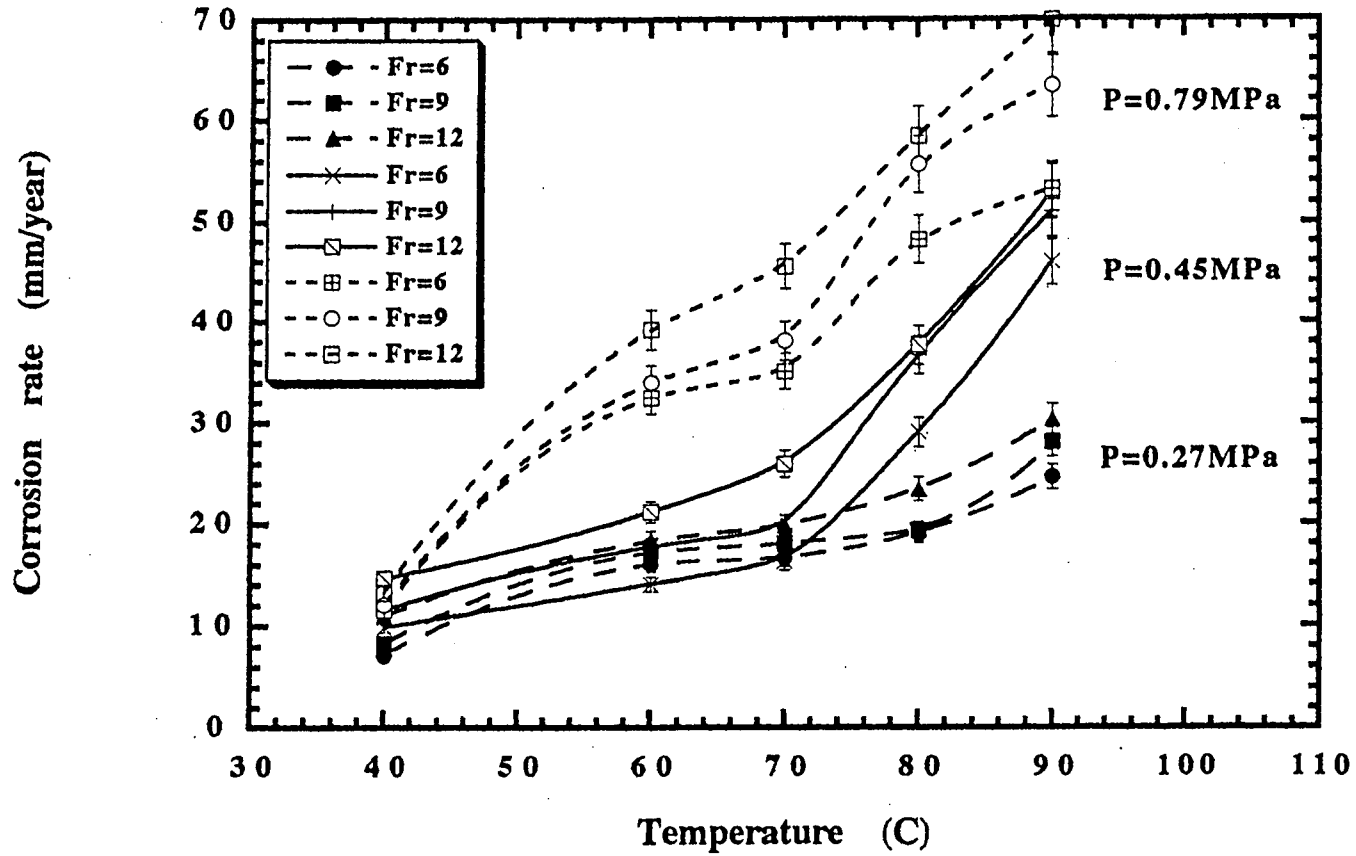


Figure 8: Variation of Corrosion Rate with Temperature for 100% Saltwater Horizontal Slug Flow

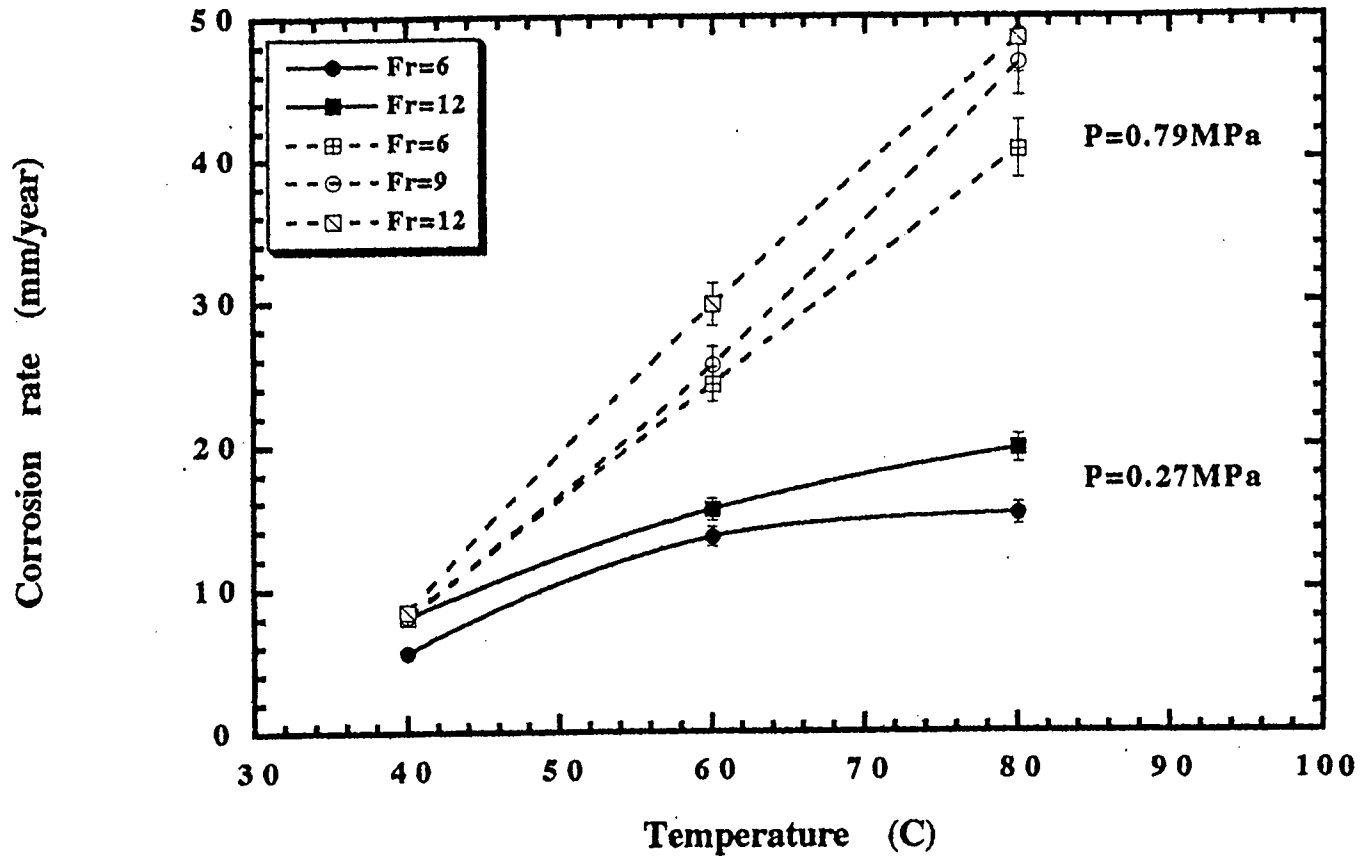
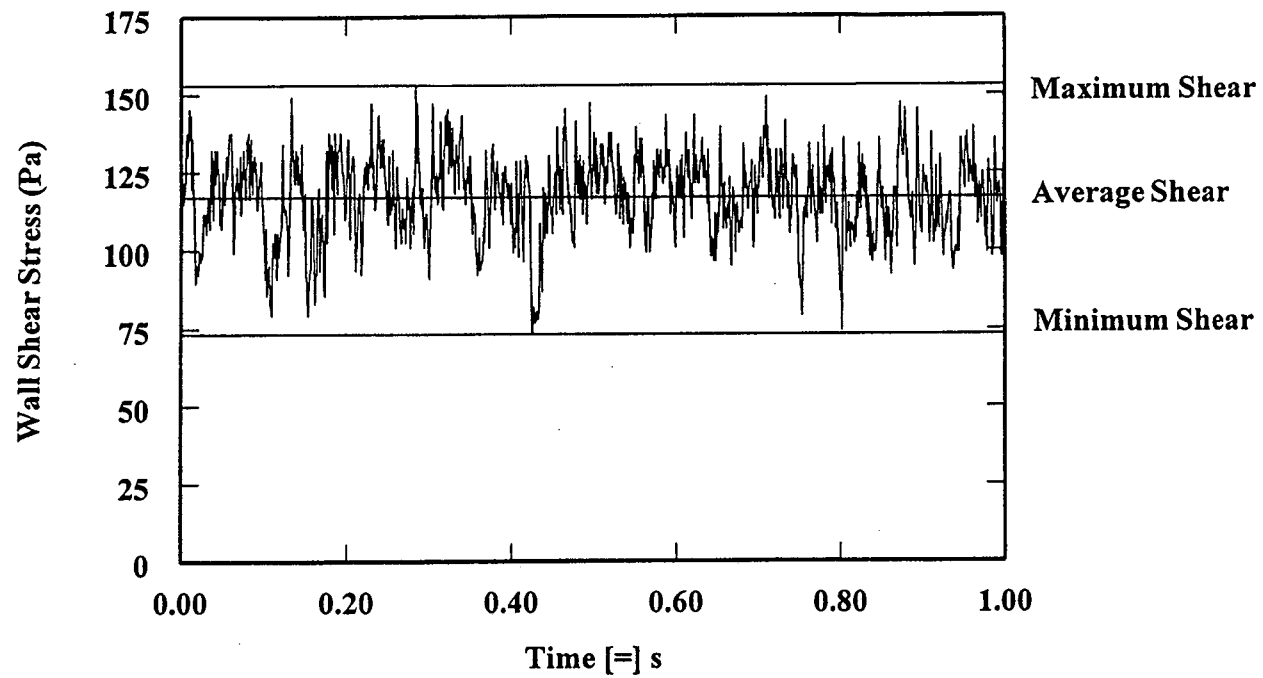
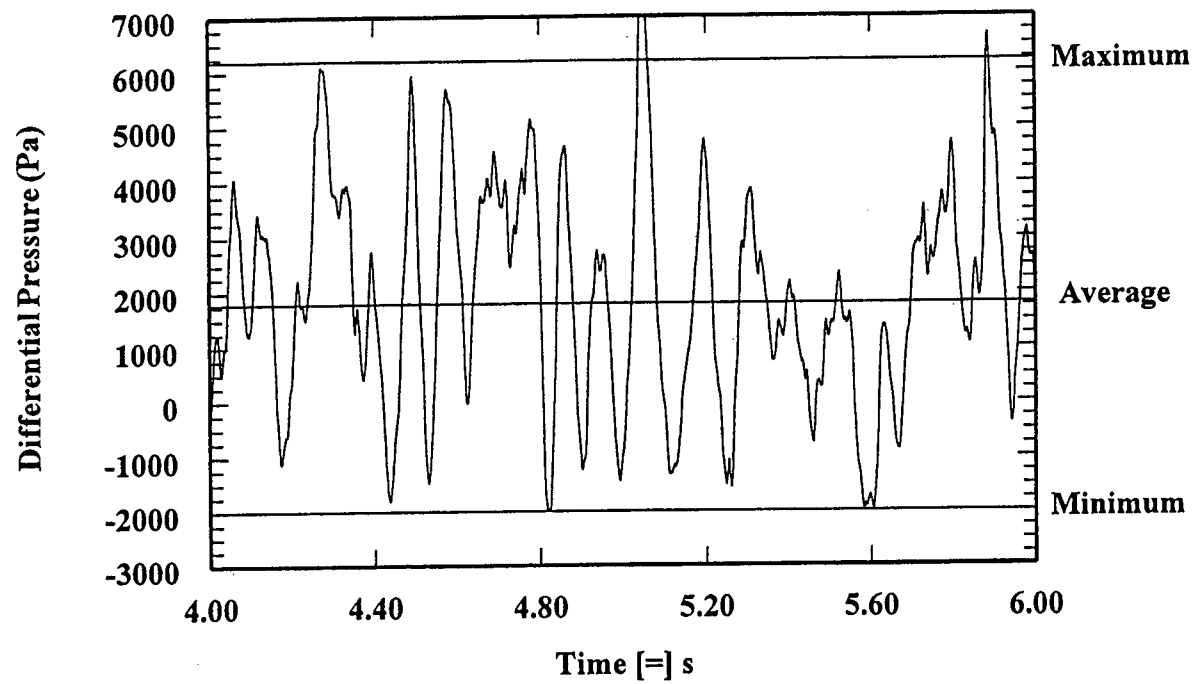


Figure 9: Variation of Corrosion Rate with Temperature for 80% Saltwater, Horizontal Slug Flow



**Figure 10: Wall Shear Stress Vs. Time for 60 cm into the slug and a film Froude number 14.0**



**Figure 11: Differential pressure Vs. Time  
60 cm into slug for film Froude number 14.0**

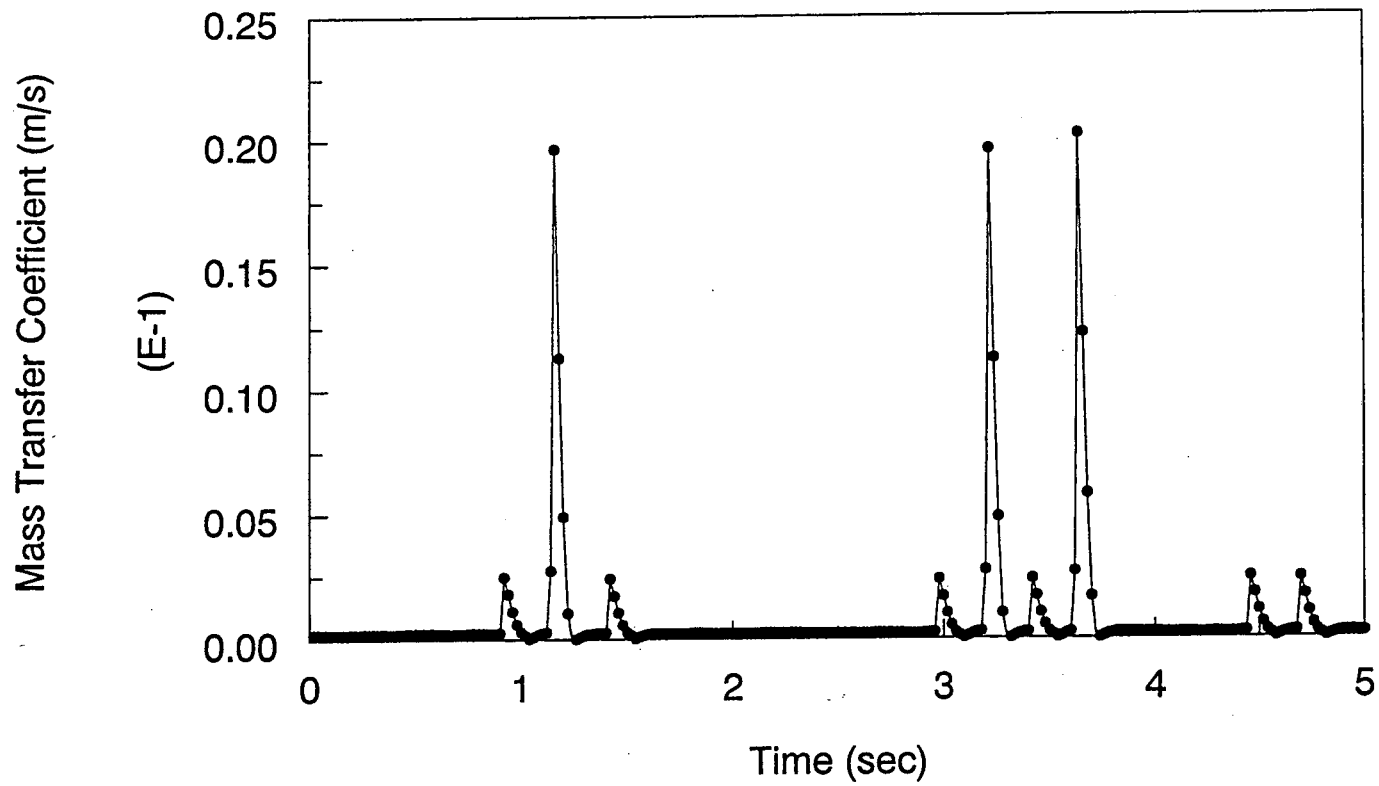


**Fig 12: Instantaneous Mass Transfer Coefficient vs Time  
for Weld Bead 1mm at Fr 11.5  
in Moving Slug Flow, Electrode #1**

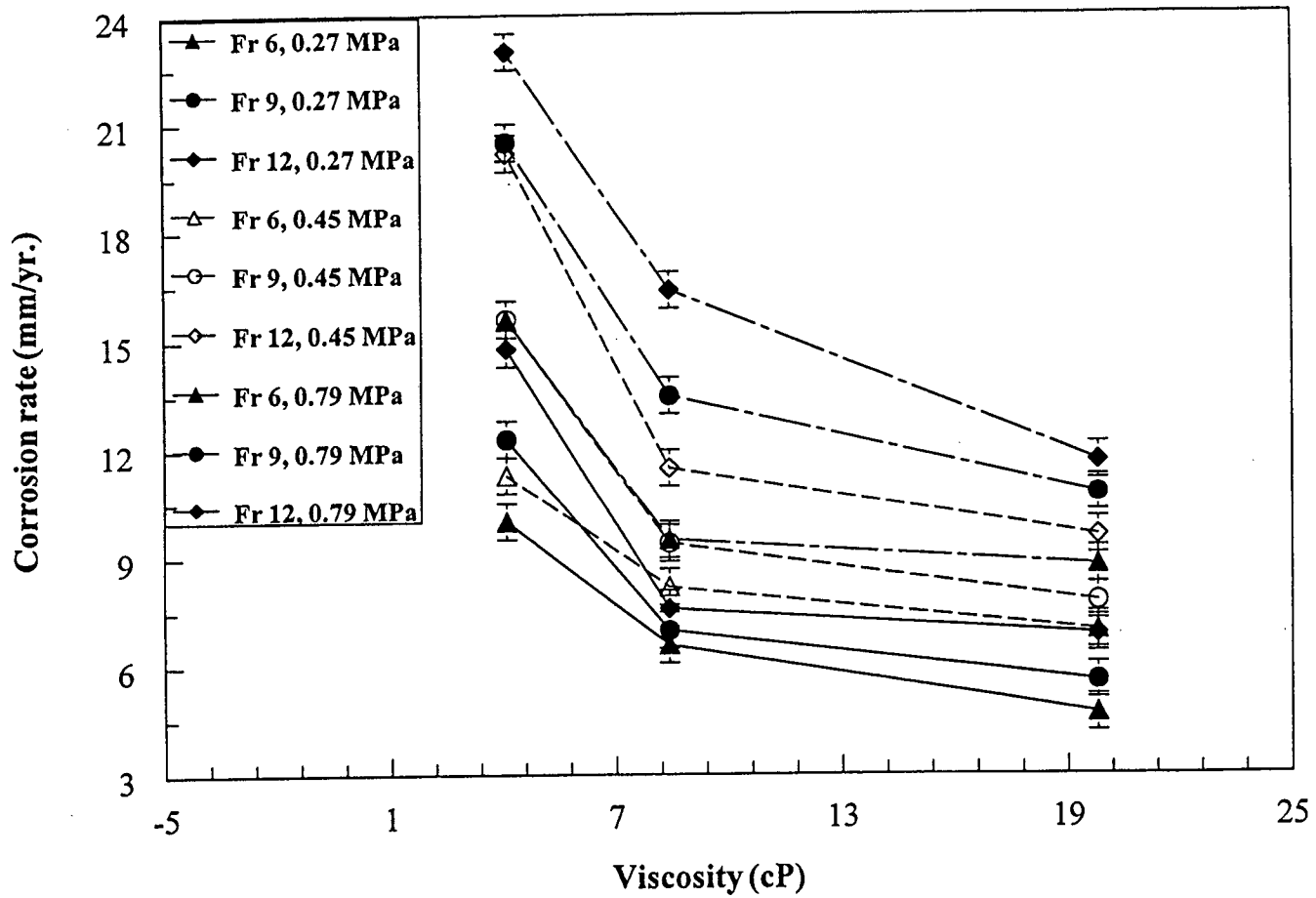
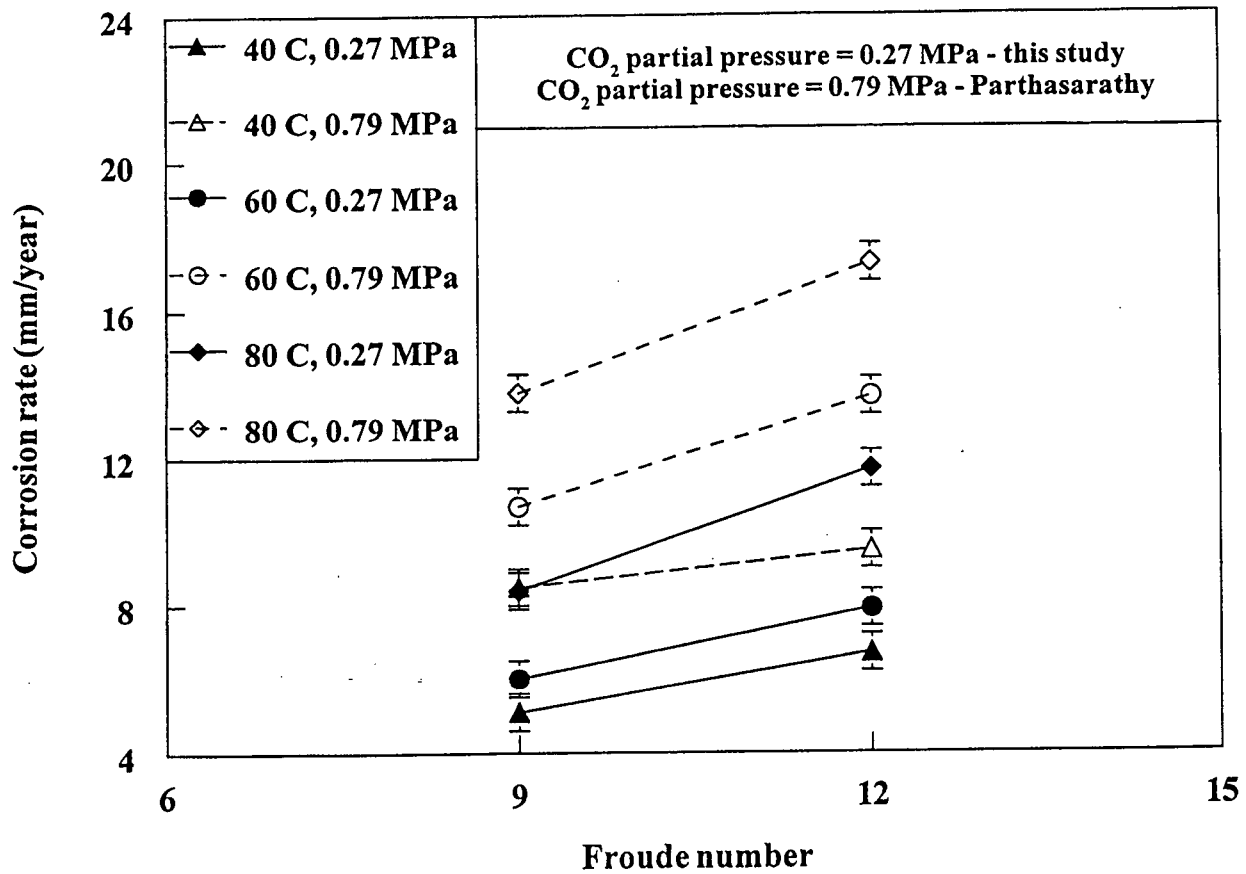


Figure 14: Effect of Viscosity on Corrosion Rate at different pressures and Froude Numbers at 80% water cut



**Figure 15: Effect of carbon dioxide partial pressure on corrosion rate at a water cut of 40 % and a constant total pressure of 0.79 MPa**

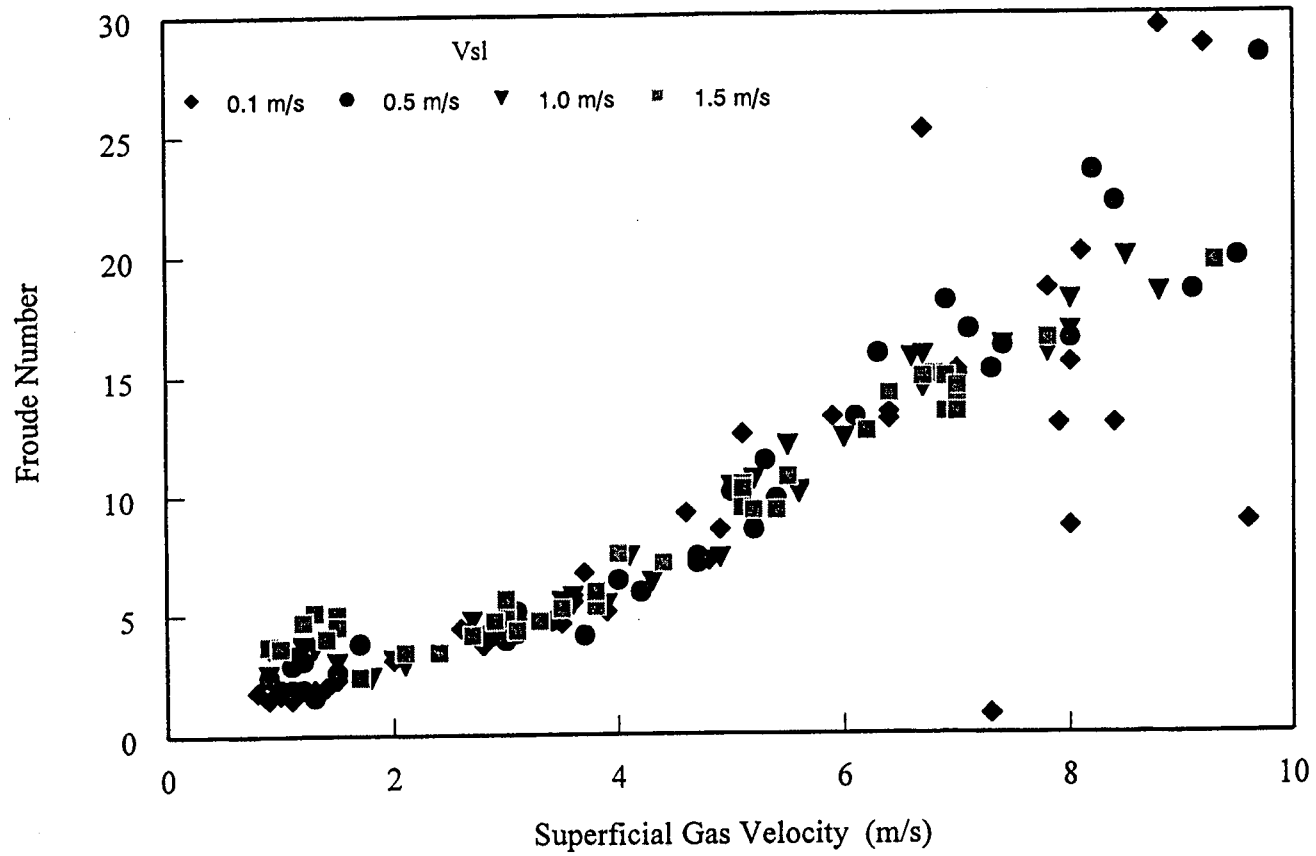


Figure 16: Froude number results @ 5° for all pressure and compositions

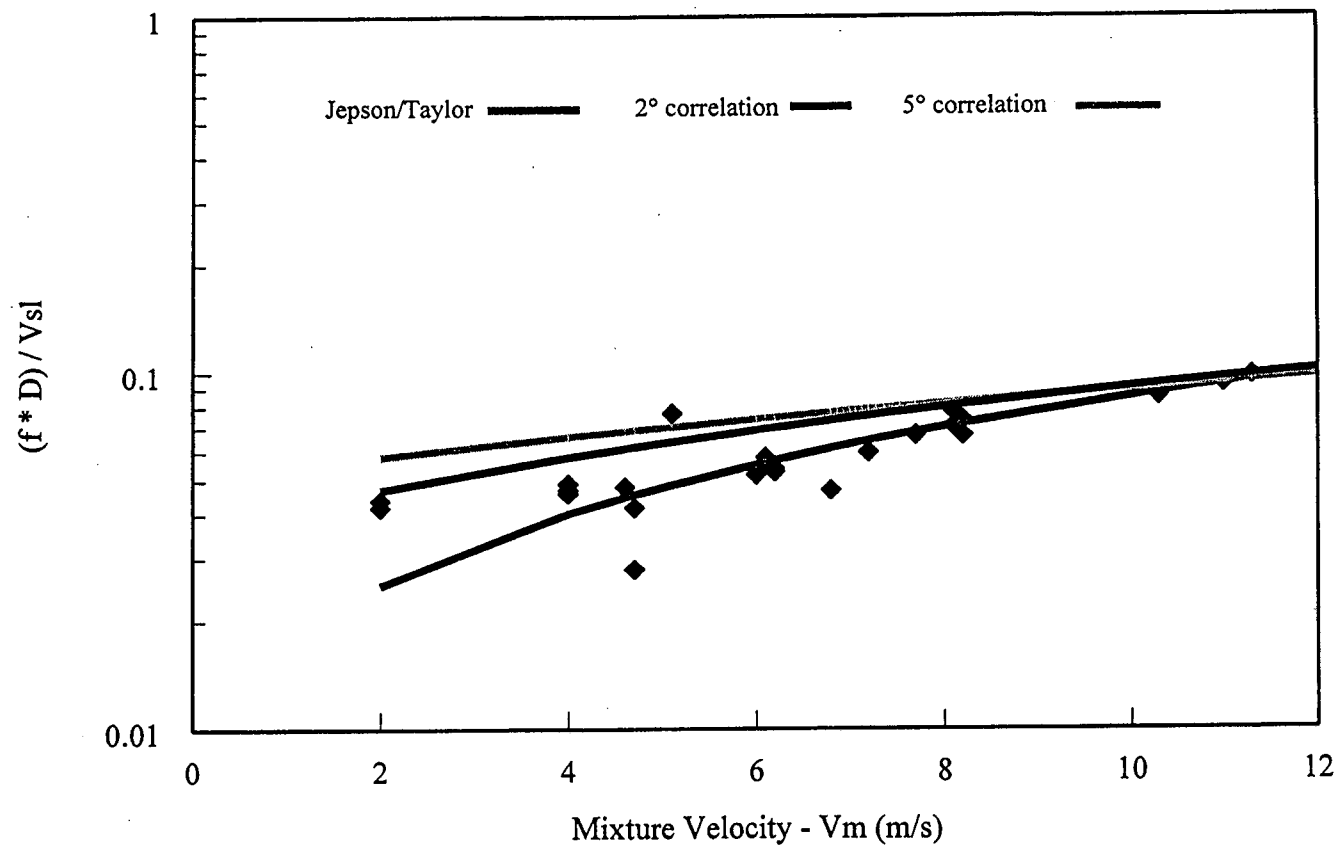


Figure 17: Jepson/Taylor (1989) results compared with the correlations developed in this study

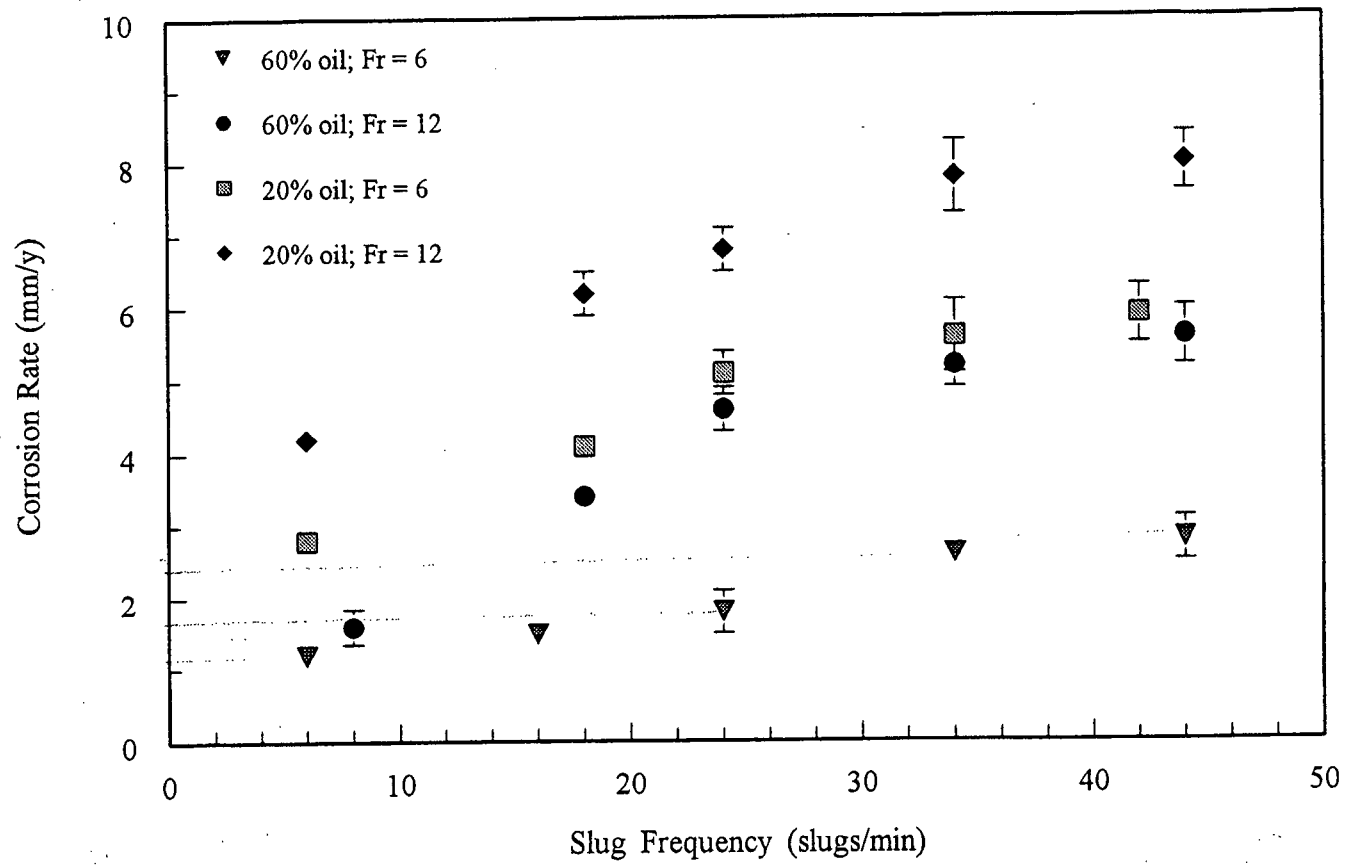


Figure 18: Variation of Corrosion Rate with Slug Frequency for 2° inclined pipes

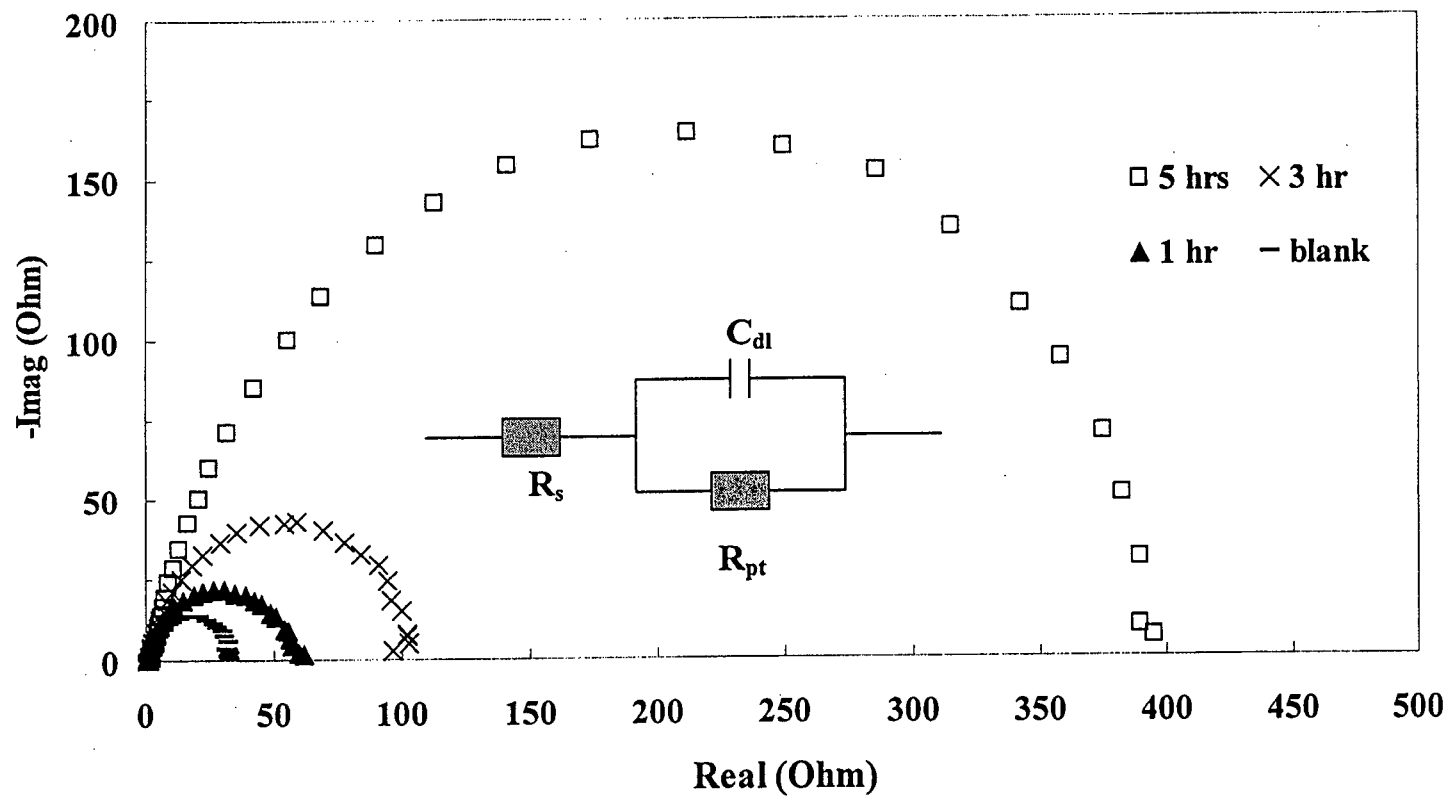


Figure 19: EIS Nyquist plots for 10ppm Package #10 in 100% watercut RCE system

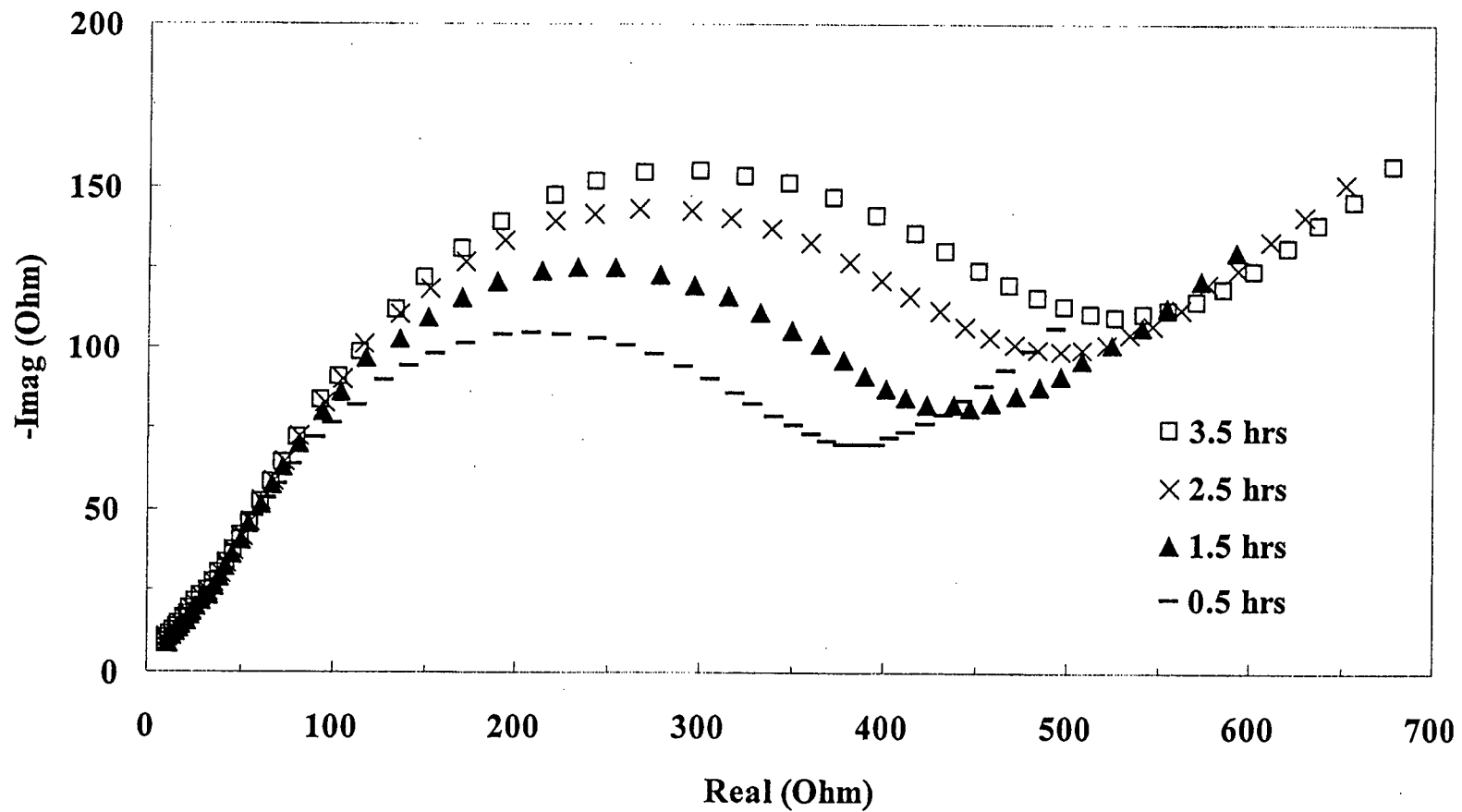


Figure 20: EIS Nyquist plots for 100ppm Package #18 in 100% watercut under Froude 9 slug flow

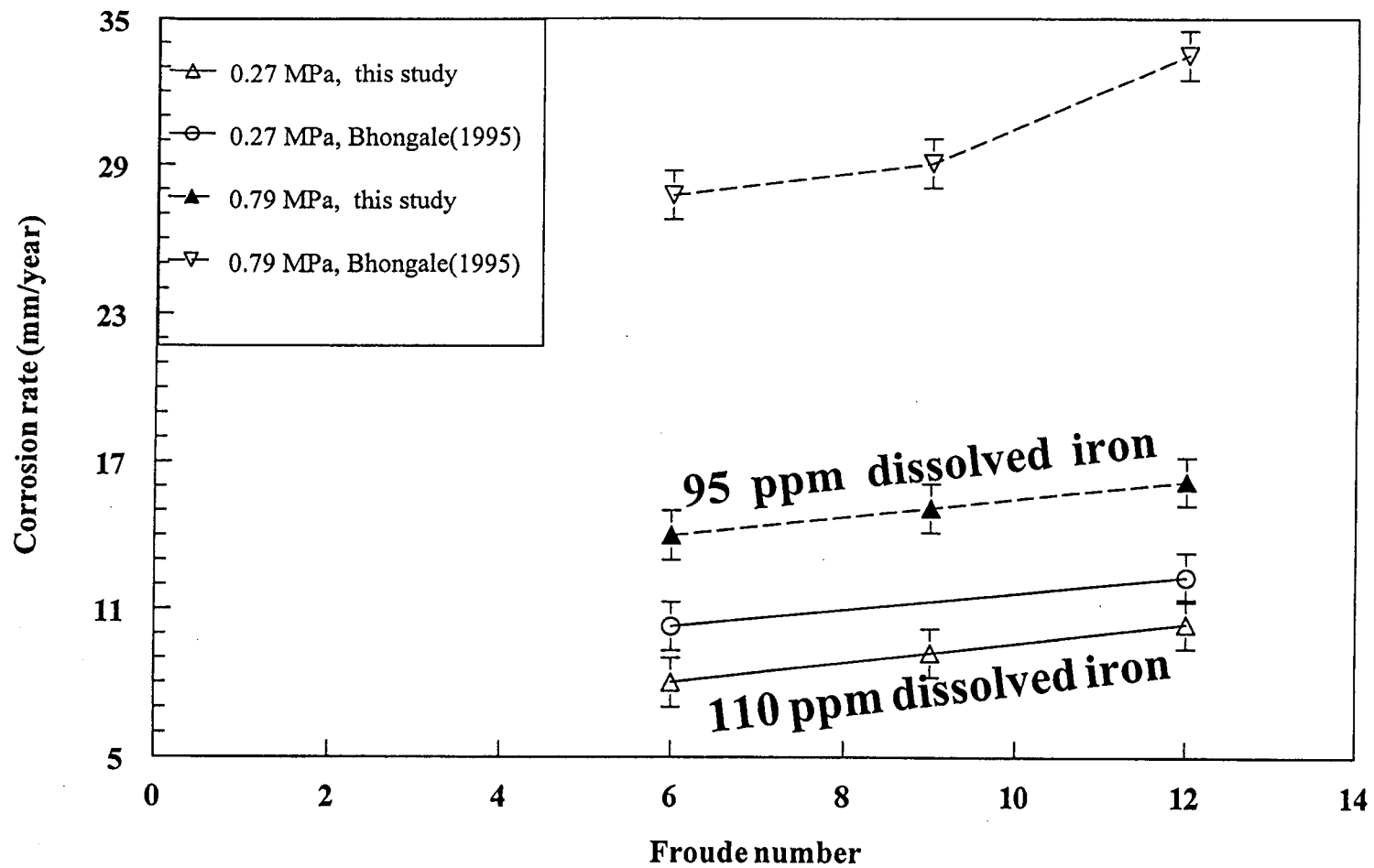


Figure 21: Comparison of corrosion rates at different pressures and Froude numbers at 40% water cut and 80 C